Eur. Phys. J. D **26**, 67–71 (2003)
DOI: 10.1140/epjd/e2003-00074-0

THE EUROPEAN PHYSICAL JOURNAL D

Laser-driven helium at 780 nm

K.T. Taylor[a], J.S. Parker, K.J. Meharg, and D. Dundas

Department of Applied Mathematics and Theoretical Physics, Queen's University Belfast, Belfast BT7 1NN, Northern Ireland, UK

Received 20 November 2002
Published online 24 April 2003 –

Abstract. We briefly review the methods under development at Queen's University Belfast to solve the full-dimensionality time-dependent Schrödinger equation for helium in intense laser fields. We set out the computational challenges involved in performing calculations that handle Ti:sapphire laser light at its fundamental wavelength (∼780 nm) in comparison to those encountered for 390 nm light. We remark upon the very considerable importance of accurate and reliable calculations at 780 nm and present results for single-ionization of helium at this wavelength.

PACS. 31.15.Ar Ab initio calculations – 31.15.Fx Finite-difference schemes – 31.70.Hq Time-dependent phenomena: excitation and relaxation processes, and reaction rates – 32.80.Wr Other multiphoton processes – 42.50.Hz Strong-field excitation of optical transitions in quantum systems; multi-photon processes; dynamic Stark shift – 02.60.Lj Ordinary and partial differential equations; boundary value problems

1 Introduction

There has been tremendous interest in recent years in the dynamics of the helium atom when exposed to the intense, short-pulse, linearly polarized radiation produced by the ubiquitous Ti:sapphire laser operating at its fundamental wavelength of ∼780 nm. We can trace this recent interest back to the dramatic experimental results for non-sequential double-ionization of this atom published by the Brookhaven group in 1994 [1]. Over the past decade there have been further important experimental findings, for example [2,3]. There has also been much theoretical effort involving classical [4] and semi-classical models [5]; reduced-dimensionality models [6]; truncated-grid finite-difference models [7]; simple building-block models [8–10], as well as analysis of experimental results to determine the contributing Feynman diagrams in S-matrix theory [11]. The common failing of all simplified theoretical models is an uncertain reliability in the *prediction* of new physics uncovered by increasingly sophisticated experimental measurement. Integration of the full-dimensionality time-dependent Schrödinger equation for the helium atom in an intense laser field is necessary to achieve this end, and, over the past decade at Belfast we have been developing numerical methods [12] to achieve accurate and reliable solutions over a wide range of laser intensity and wavelength.

High accuracy numerical solutions of the time-dependent helium Schrödinger equation have a wealth of important applications in both theoretical and experimental atomic physics. First they enable the calculation of intense-field (two-electron) phenomena that no reduced-dimensionality or *ad hoc* theory can adequately model, as for example double-electron ATI, which was first predicted and described in [13]. Second they provide guidance in the design of simplified theoretical models of multi-electron, atom-laser interactions [14,15]. Third, they enable reliable, and often predictive, calculation of high-accuracy data of immediate experimental relevance. An example is the angular resolution of non-sequential double-ionization which such calculation [16] demonstrated (in advance of laboratory experiment) to involve both electrons leaving the atom on the *same* side of the nucleus. However the most crucial such calculations in recent years have yielded cross-sections for single- and double-electron ionization, for a laser wavelength of 390 nm, that enable experimentalists to accurately determine laser intensities for the frequency-doubled Ti:sapphire laser [17].

For the past few years we have been making further developments to our algorithms and numerical methods so that full advantage can be taken of the steadily growing power and memory of supercomputers. These advances now start to make accurate and reliable calculations for a laser wavelength of 780 nm possible for the first time.

In the sections below we first briefly describe our method for solving the full-dimensionality time-dependent Schrödinger equation for this problem. Following this, we point out the much greater difficulties involved with handling 780 nm compared to those encountered with 390 nm radiation, but we also emphasise the various important

[a] e-mail: k.taylor@qub.ac.uk

benefits that accrue from accurate and reliable calculations specifically for this longer wavelength. Illustrative results from our 780 nm calculations in the form of single ionization rates are then presented where the role of a Single Active Electron model in establishing the convergence of such results is demonstrated. Further developments are mentioned in a concluding section.

2 Belfast method for helium

To perform the integration [12] of the TDSE for laser-driven helium Parker *et al.* use a mixed basis set, finite-difference (FD) method, in which the two radial coordinates r_1 and r_2 are modelled on a finite-difference grid, and the four angular coordinates $\theta_1, \theta_2, \phi_1, \phi_2$ are handled by writing the wavefunction on a basis set of coupled spherical harmonics or partial waves, $|l_1 l_2 LM\rangle$. In linearly polarised light, the z-component of the total angular momentum, M, is constant resulting in only 5 independent spatial-dimensions. The interaction of each electron with the laser light is represented using the velocity form of the electric dipole operator. Since the initial state has $M = 0$, the wavefunction $\Psi(r_1, r_2, \theta_1, \theta_2, \phi_1, \phi_2, t)$ is written as,

$$\Psi = A \sum_{L,l_1,l_2} f_{L,l_1,l_2}(r_1, r_2, t)\, |l_1 l_2 L\rangle\,, \qquad (1)$$

where A is the Pauli symmetrisation operator. Electron spin S is conserved: in the present case of a singlet initial state, $S = 0$ at all times, so that A enforces even symmetry of the wavefunction under exchange of electron spatial coordinates.

The radiation field has the freedom to exchange angular momentum with the electrons, and the number of partial waves coming into play can become quite large. The largest number of partial waves used to date is 3800. With this setting, the Schrödinger equation becomes a set of 3800 coupled two-dimensional time-dependent, partial differential equations, each of which is solved by FD techniques. The differential operators of the atomic Hamiltonian are approximated as 5 point FD operators.

The basis state decomposition is particularly well suited to parallel machines. The present version of the code runs well on such machines including the Cray T3E-1200E used in the largest calculations. The less demanding problems (at high laser frequencies for example) can now run efficiently on single processor personal computers.

An absorbing potential at the outer boundary is not used but rather the wavefunction is split into a coherent superposition of an outer part and an inner part. The outer part is zero at small radial distances but grows so that it contains the total wavefunction at the outer boundary, with the consequence that the inner part smoothly approaches zero at the boundary. At present this outer part is discarded and so the net effect is equivalent to that of an absorbing boundary.

The numerical method is capable of faithfully modelling double ionization, autoionisation, or any other effect associated with highly correlated states of the two electrons. The degree to which the numerical integration approximates the Schrödinger equation is governed by four parameters in the code: the spacing, δr, of the finite-difference grid points representing the two radial variables; the maximum angular momentum of each electron $l_{\max}$ present in the partial-wave expansion; the number of terms retained in a series expansion of the electron-electron interaction, N; and the size of the integration volume, R. Choosing appropriate values for these parameters can make the model arbitrarily close to the Schrödinger equation from which it is derived.

The Belfast two-electron atomic code, HELIUM, also incorporates three arbitrary parameters that ensure the bound state energies on the FD grid are correct to 0.02% or better, independently of δr, (the grid point separation). Thus three states are shifted to their correct energies: the ground state of He, the ground state of He^+, and the $1s2p\ ^1P^o$ state. These three states are ordinarily the most poorly represented by the FD grid. They are the three lowest energy states, and because they lie within a few Bohr (au) of the nucleus they span relatively few of the discrete grid points. No other states require adjustment. All the other states span a far greater number of grid points, are insensitive to the Laplacian boundary parameter, and are well represented by the grid.

Over the past few years the method has been applied to one-electron ionization where it has been used to develop a quantitatively accurate Single Active Electron (SAE) model [14,18]. Also, under laser intensities that bring about only single ionization, results generated have been found to be in close agreement [15] with those obtainable from the R-matrix Floquet approach. It has also yielded [17], for a laser wavelength of 390 nm, the first direct comparison of experimental results at optical frequencies for double ionization [19] with those from a reliable and accurate model.

3 Calculation demands of 780 nm

A doubling of the laser wavelength from 390 nm to 780 nm brings about a huge increase in the computational effort that is needed to effect an accurate and reliable calculation at any given laser intensity.

The first point to note is that since each photon now carries half as much energy, a greater number will need to be absorbed to bring about single (or double) ionization of the atom. Given that each photon absorption can bring about a unit change in electronic angular momentum quantum number we can thus expect that a larger upper limit on both l_1 and l_2 (and hence also on L) will have to be retained in equation (1).

The second point bears on the fact that for a given intensity the quiver amplitude α_0 associated with free electron motion in a laser field is proportional to the square of the laser wavelength. Thus the quiver amplitude of electronic motion driven by a 780 nm laser is four times that brought about by a 390 nm laser at the same operating intensity. To handle this quadrupling in a calculation requires a considerable increase in the box size in both r_1

Table 1. Quiver amplitudes and ponderomotive energies for a range of intensities of 780 nm radiation.

Intensity (10^{14} Wcm^{-2})	α_0 (a.u.)	$3.17U_\mathrm{p}$ (a.u.)
1.0	15.64	0.66
2.0	22.12	1.32
4.0	31.29	2.65
6.0	38.32	3.97
8.0	44.25	5.29

and r_2. Some values of α_0 over the intensity range of interest for 780 nm radiation are given in Table 1.

These first two points bring about a very substantial increase in computer memory requirements together with a commensurate increase in number of arithmetic operations and communications overhead in each time-step of the wavefunction propagation.

The third point is that a laser cycle at 780 nm has twice the time-period of one at 390 nm. To maintain an accurate description of the physics we cannot significantly increase the mesh-spacing in r_1 and r_2 and thus cannot significantly alter the size of time-step. Thus twice as many time-steps must be propagated to cover a cycle of 780 nm radiation as is required for a cycle at 390 nm.

4 Benefits from a calculation at 780 nm

There are at least three major benefits from a direct integration of the TDSE for helium exposed to 780 nm radiation.

The first is that such a calculation can give reliable direct temporal information on the double (and single) ionization processes. This gives extra insight on such processes and allows the validity of simple models to be tested.

The second is that as one increases laser intensity at this wavelength over the range experimentally achievable, one goes from one extreme to the other of the simple classical recollision model [20]. Thus, see Table 1, at 1.0×10^{14} W/cm^2 we have $3.17U_\mathrm{p} = 0.66$ Hartrees whereas at 6.0×10^{14} W/cm^2 we have $3.17U_\mathrm{p} = 3.97$ Hartrees. In the former case (1.0×10^{14} W/cm^2), according to the simplest classical recollision model [20], the returning electron has insufficient energy to either ionize the remaining electron from the He^+ ground state (bound by 2.0 Hartrees) or to excite it from the He^+ ground state to the first excited states (energy gap of 1.5 Hartrees). In the latter case (6.0×10^{14} W/cm^2), however, the maximum return energy of $3.17U_\mathrm{p}$ is more than sufficient to ionize He^+ from its ground state.

The third major benefit is that such a calculation is independent of guidance from any particular laboratory experiment. It does *not* play the *post facto* role of other calculations (even by some described as *ab initio*) of simply analysing and explaining data already obtained in the laboratory.

5 The SAE model for helium

As explained above, in the limit of long wavelengths, it becomes increasingly expensive to use optimal settings for the four integration parameters that govern the degree to which the helium numerical integration accurately models the true Schrödinger equation; namely δr, l_max, N and R. We turn now to a discussion of techniques we have developed to extrapolate numerical results to more accurate values, and of equal importance, techniques we have developed to reliably estimate errors induced by the numerical model.

The extrapolation and error estimates are performed by using a Single Active Electron (SAE) model of single electron ionization of helium [14]. The SAE model is based on a static (screened Coulomb) potential with the same ionization potential as helium.

The SAE model was originally developed in order to explore the basics physics of single electron ionization, by testing the assumption that the two electrons can be decorrelated during this process. In the present problem, we will be using the SAE to obtain more accurate calculations of physical quantities.

Toward this end, we exploit two parameters that appear in the SAE formulation. With a single setting of these two numbers, the SAE model can be tuned to give near quantative agreement with HELIUM ionization rates over the range of $1-14\times10^{14}$ W/cm^2. In most cases, the agreement is within 1%. The SAE implementation shares with the HELIUM code three of the four integration parameters; δr, l_max and R. Because the SAE models only one electron, it is two orders of magnitude faster than the HELIUM code and for this reason we can choose highly optimal settings for δr, l_max and R.

Once the SAE has been tuned to the HELIUM results, and once we have verified that the SAE and HELIUM methods converge at the same rate as the parameters are varied, the SAE can then be used to extrapolate to the limit of small δr, large l_max and R and long duration pulses. We turn now to an example that illustrates the method at 780 nm.

6 Use of SAE model at 780 nm

Figure 1 shows the case of 16-photon single electron ionization of helium. The HELIUM and SAE results (obtained with identical values of l_max, δr and R) are nearly indistinguishable over 18 field periods. The figure shows population within 12 Bohr of the nucleus as a function of time – tick marks on the population axis are labelled with values corresponding to 1.0 minus the near-unity population remaining within 12 Bohr. In typical cases population leaves this region at a net constant rate and the data averaged over several field periods would be a straight line.

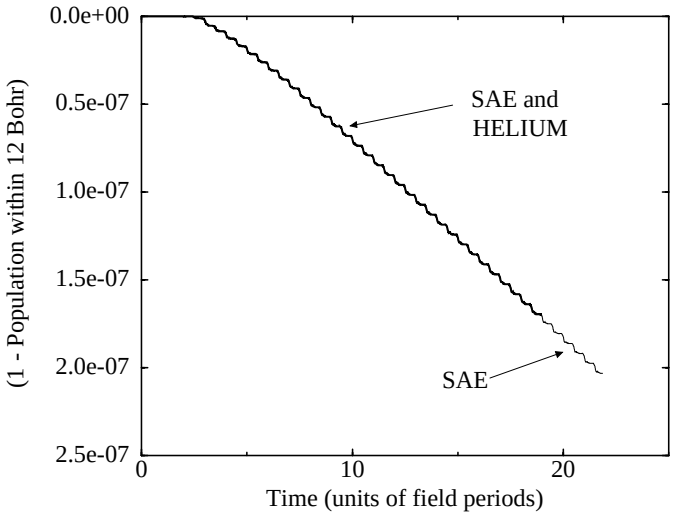

Fig. 1. Comparison of population curves generated from the HELIUM and SAE codes at an intensity of 1×10^{14} W/cm^2 for a laser of 780 nm. The initial state is the $1s1s$ ground state of helium.

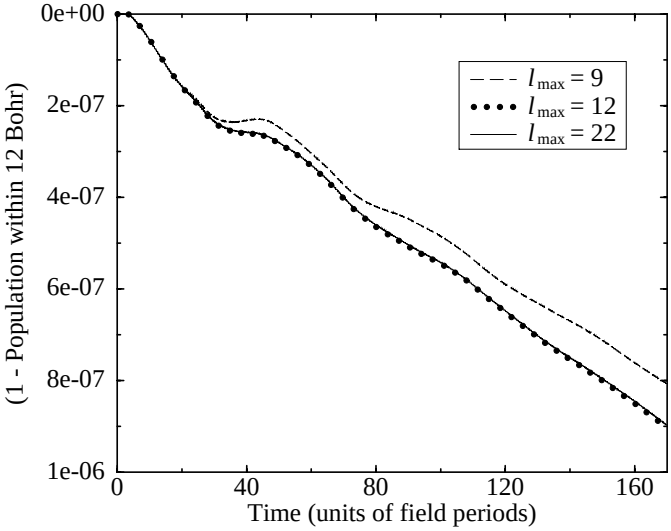

Fig. 2. Population curves for the same laser parameters as in Figure 1, but from the SAE model for differing choices of $l_{\max}$.

In the case of Figure 1 a certain curvature over several field periods is clearly evident early on, which is evidence of strong resonances with a bound states. For example, an estimate of the Stark shift of the ground state suggests that there is a (near) 17-photon resonance with the $1s2p$ state. The effect of these resonances will dramatically alter the dynamics as we integrate further in time.

An important incidental point to note from the figure is that the initial state is depleted by only a few parts in 10^{-7} during the course of the integration. It follows that the wavefunction must be integrated with truncation errors substantially below 10^{-7} which places severe constraints on the design of the time propagator. The problem is even more serious in calculations of double ionization which occurs at rates several orders of magnitude smaller than that of single electron ionization. Our solution to this difficulty is discussed in [12].

In Figure 2 we show the results of a 170 field period integration of the SAE model with the same physical parameters as pertained to Figure 1. The strong influence of resonant bound states is clearly evident, but it is also apparent that by 170 field periods, transients have died away and the ionization rate has approached a constant. The comparatively rapid depletion of the helium ground state at the beginning of the pulse, followed by a long interval at an inhibited ionization rate is characteristic of a resonant process suggested in more detail in [15].

Figure 2 also shows convergence of the results as the basis set of partial waves increases in size with $l_{\max}$. The results at $l_{\max} = 12$ differ only by a few percent from the converged results at $l_{\max} = 22$. Results at $l_{\max} = 16$, not shown, are indistinguishable from those at $l_{\max} = 22$. In practice all HELIUM calculations are performed at $l_{\max} = 16$, and at selected cases the calculations are performed at $l_{\max} = 12$. We then verify that the SAE results converge at the same rate as the HELIUM results as $l_{\max}$ changes from 12 to 16. We can then accept with some confidence that the converged SAE results are more accurate than the HELIUM results. The distance between the converged SAE results and the HELIUM results is taken as an estimate of the uncertainty in the calculation.

7 Conclusions

The methods we have developed in Belfast (and implemented in the computer code HELIUM) for reliably and accurately integrating the full-dimensionality Schrödinger equation describing the helium atom exposed to intense laser pulses are at the point of yielding definitive results for the important laser wavelength of 780 nm. We have illustrated this here with single ionization rates whose quality has been established against an SAE model as appropriate.

Results for double ionization rates as well as assessment of simple tunnelling models [21] will be reported in future publications.

This work in this paper is supported in part by the UK Engineering and Physical Sciences Research Council by provision of financial support for JSP and DD, as well as resources used at the Computer Service for Academic Research. KJM acknowledges receipt of a studentship award from the Northern Ireland Department of Employment and Learning (formerly DHFETE).

References

1. B. Walker, B. Sheehy, L.F. DiMauro, P. Agostini, K.J. Schafer, K.C. Kulander, Phys. Rev. Lett. **73**, 1227 (1994)
2. T. Weber, M. Weckenbrock, A. Staudte, L. Spielberger, O. Jagutzki, V. Mergel, F. Afaneh, G. Urbasch, M. Vollmer, H. Giessen, R. Dörner, Phys. Rev. Lett. **84**, 443 (2000)

3. R. Lafon, J.L. Chaloupka, B. Sheehy, P.M. Paul, P. Agostini, K.C. Kulander, L.F. DiMauro, Phys. Rev. Lett. **86**, 2762 (2001)
4. B. Feuerstein, R. Moshammer, J. Ullrich, J. Phys. B: At. Mol. Opt. Phys. **33**, L823 (2000)
5. S.P. Goreslavskii, S.V. Popruzhenko, R. Kopold, W. Becker, Phys. Rev. A **64**, 053402 (2001)
6. C. Szymanowski, R. Panfili, W.C. Liu, S.L. Haan, J. Eberly, Phys. Rev. A **61**, 055401 (2000)
7. H.G. Muller, Opt. Expr. **8**, 417 (2001)
8. S.P. Goreslavski, S.V. Popruzhenko, Opt. Expr. **8**, 395 (2001)
9. J.B. Watson, A. Sanpera, D.G. Lappas, P.L. Knight, K. Burnett, Phys. Rev. Lett. **78**, 1884 (1997)
10. H.W. van der Hart, J. Phys. B: At. Mol. Opt. Phys. **33**, L699 (2000)
11. A. Becker, F.H.M. Faisal, Opt. Expr. **8**, 383 (2001)
12. E.S. Smyth, J.S. Parker, K.T. Taylor, Comput. Phys. Commun. **114**, 1 (1998)
13. J.S. Parker, L.R. Moore, K.J. Meharg, D. Dundas, K.T. Taylor, J. Phys. B: At. Mol. Opt. Phys. **34**, L69 (2001)
14. J.S. Parker, E.S. Smyth, K.T. Taylor, J. Phys. B: At. Mol. Opt. Phys. **31**, L571 (1998)
15. J.S. Parker, D.H. Glass, L.R. Moore, E.S. Smyth, K.T. Taylor, P.G. Burke, J. Phys. B: At. Mol. Opt. Phys. **33**, L239 (2000)
16. K.T. Taylor, J.S. Parker, D. Dundas, E. Smyth, S. Vivirito, Laser Phys. **9**, 98 (1999)
17. J.S. Parker, L.R. Moore, D. Dundas, K.T. Taylor, J. Phys. B: At. Mol. Opt. Phys. **33**, L691 (2000)
18. J.S. Parker, L.R. Moore, E.S. Smyth, K.T. Taylor, J. Phys. B: At. Mol. Opt. Phys. **33**, 1057 (2000)
19. B. Sheehy, R. Lafon, M. Widmer, B. Walker, L.F. DiMauro, Phys. Rev. A **58**, 3942 (1998)
20. P.B. Corkum, Phys. Rev. Lett. **71**, 1994 (1993)
21. M.V. Ammosov, N.B. Delone, V.P. Krainov, Sov. Phys. JETP **64**, 1191 (1986)